

# Coherent anti-Stokes generation from single nanostructures

Hyunmin Kim<sup>a</sup>, Tatyana Sheps<sup>b</sup>, David K. Taggart<sup>a</sup>, Philip G. Collins<sup>b</sup>, Reginald M. Penner<sup>a</sup>  
and Eric O. Potma<sup>a</sup>

<sup>a</sup>Department of Chemistry, University of California, Irvine, USA;

<sup>b</sup>Department of Physics and Astronomy, University of California, Irvine, USA

## ABSTRACT

Dual color four-wave-mixing is used to visualize individual gold nanowires and single carbon nanotubes. The strong nonlinear signals, which are detected at the anti-Stokes frequency, originate from the electronic response of the nanostructures. In gold nanowires, the collective electron motions produce detectable coherent anti-Stokes signals that can be used to study the orientation and relative strength of the structure's plasmon resonances. In single walled carbon nanotubes, coherent anti-Stokes contrast can be used to map the orientation of the electronic resonances in single tubes. Coherent anti-Stokes imaging of the material's electronic response allows the first close-ups of the coherent nonlinear properties of individual structures and molecules.

**Keywords:** Four wave mixing, coherent anti-Stokes Raman scattering, nanostructure, carbon nanotubes

## 1. INTRODUCTION

The popularity of coherent anti-Stokes Raman scattering (CARS) as an optical probing technique originates from its sensitivity to molecular vibrational modes.<sup>1</sup> Nonetheless, the CARS technique probes such nuclear vibrations indirectly through the motions of the material's electrons, which are the primary source of radiation. The intrinsic electronic character of the CARS process also dresses the technique with an infamous nonresonant background, i.e. anti-Stokes radiation that results purely from electron motions, which are independent of the presence of nuclear modes. This purely electronic contribution, often indicated by the material's nonresonant nonlinear susceptibility  $\chi_{nr}^{(3)}$ , introduces a background and mixes coherently with the anti-Stokes radiation originating from the presence of vibrational resonances ( $\chi_{nr}^{(3)}$ ). In the field of CARS microscopy, a vast amount of work has been devoted to suppressing the  $\chi_{nr}^{(3)}$  signal contributions, and alternative coherent Raman methods have been suggested that avoid the generation of purely electronic signals all together.

Despite the bad reputation of the  $\chi_{nr}^{(3)}$  terms, the purely electronic response in a coherent anti-Stokes experiment can be used as a useful probe for the nonlinear optical properties of a variety of materials. In particular, many structures at the nanoscale exhibit unusually high electronic polarizabilities, which produce strong  $\chi_{nr}^{(3)}$  signals. These strong coherent anti-Stokes signatures can be used not only to visualize single nanostructures and nanotubes, but also to determine the nonlinear optical characteristics of such single structures and compounds.

In this contribution we demonstrate optical imaging based on the nonlinear  $\chi^{(3)}$  response of nanostructures. In analogy with CARS microscopy, we will probe the  $\chi^{(3)}$  response by detecting the coherent anti-Stokes emission. However, instead of focusing on the Raman vibrational response of the target structures, we will be primarily concerned with their electronic optical properties. We show that this approach allows a direct mapping of plasmon resonances in single gold nanowires. In addition, we report that coherent anti-Stokes detection is a sensitive method for examining the coherent electronic response of single carbon nanotube molecules.

---

Further author information: (Send correspondence to E.O.P.)

E.O.P.: E-mail: epotma@uci.edu

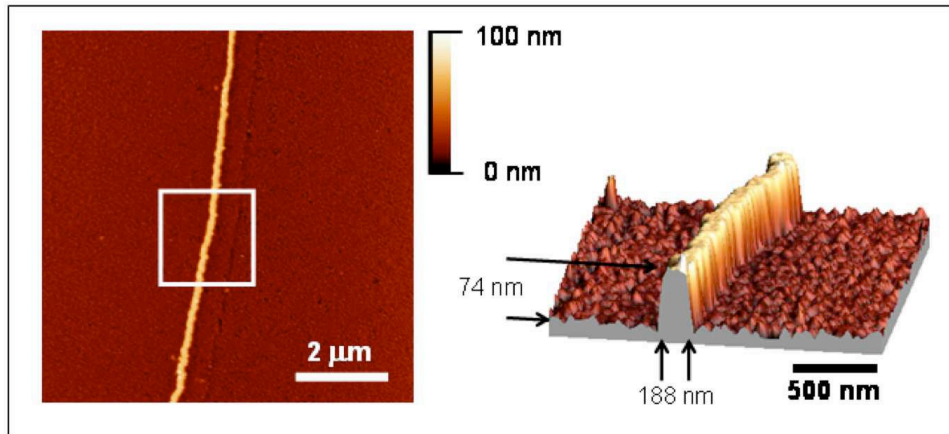


Figure 1. Atomic force micrograph of a single gold nanowire ( $w = 188$  nm;  $h = 74$  nm) fabricated with lithographically patterned nanowire electrodeposition.

## 2. COHERENT EMISSION FROM METALLIC NANOSTRUCTURES

Surface plasmons resonances (SPR) are collective electron motions at metal surfaces. In several materials, most notably gold, these collective resonances can be excited with optical radiation in the visible range. The collective electron motions produce a local electric field that oscillates at the resonance frequency. The local electric fields are typically much stronger than the optical driving field, and can significantly enhance the optical response of the material near the surface. Besides strong linear optical signals, the surface plasmon resonances have also been shown to exhibit a strong nonlinear optical response. In 1979, Chen and coworkers demonstrated enhanced dual color ( $\omega_1, \omega_2$ ) four-wave-mixing at metallic surfaces, detected at the anti-Stokes frequency ( $2\omega_1 - \omega_2$ ).<sup>2</sup> The strong coherent emission was attributed to the nonlinear response of the surface electrons.

Plasmon resonances are also prominent in metallic nanostructures. It is well known that gold and silver nanostructures in the 10 to 100 nm range have surface electron resonances in the visible range of the spectrum. Compared to SPR at macroscopic surfaces, the plasmon resonances in nanostructures can be driven under relaxed wave vector matching conditions. The strong local electric fields associated with these resonances can be used to enhance optical effects in the vicinity of the metallic interface, most notably the Raman response of molecules attached to the surface. Surface enhanced Raman scattering (SERS), for example, is an enormously popular technique for detecting molecular compounds at low concentrations with vibrational spectroscopic selectivity.

The collective electron motions in nanostructures can also be the source for nonlinear optical signals. In 1983, Chemla *et al* recorded  $\chi^{(3)}$  induced signals from an array of silver nanoparticles.<sup>3</sup> The four-wave-mixing signals were generated through the combined action of a pump ( $\omega_1$ ) and a Stokes ( $\omega_2$ ) driving field, and detected at the anti-Stokes frequency ( $2\omega_1 - \omega_2$ ). More than two decades later, similar signals were attained from isolated gold nanoparticles<sup>4</sup> and individual gold nanowires.<sup>5</sup> In the following two sections, using nanowires as our model system, we will discuss how the electronic coherent anti-Stokes signal can be used to study the orientation and associated enhanced local fields of plasmon resonances in metallic nanostructures.

## 3. OPTICAL PROPERTIES OF GOLD NANOWIRES

Gold nanowires are elongated nanostructures with precisely defined dimensions. Using lithographic electrodeposition techniques, wires with a length on the order of centimeters can be fabricated, whereas the width and height of the wires are controllable within the 10 - 500 nm range.<sup>6</sup> Because the long axis is of macroscopic dimensions, such structures are ideal model systems for studying the orientation dependent nonlinear optical properties of plasmon resonances using a far field microscope. In addition, the controllable width and height of the nanowires permits a detailed study of how the nonlinear response of the plasmon resonance scales with size and shape.

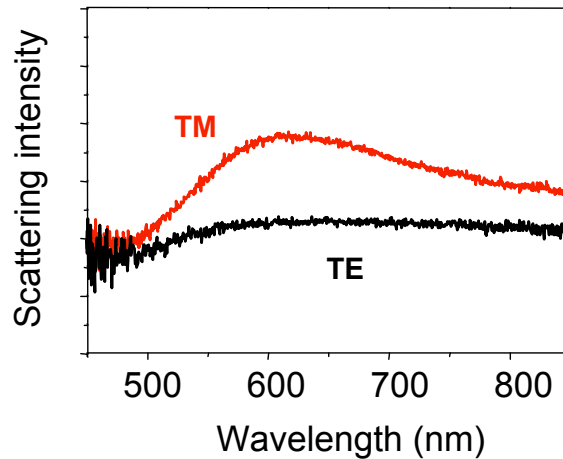


Figure 2. White light scattering spectrum of a single gold nanowire ( $w = 188$  nm;  $h = 74$  nm) measured using an epi-detected geometry for capturing the scattered light with a high numerical objective. TM denotes the situation when the incident light is perpendicularly polarized to the longitudinal axis of the nanowire and TE when it is parallel.

An atomic force micrograph of a gold nanowire sample is shown in Figure 1. The width of this wire is 188 nm and the height is 74 nm. Figure 2 shows the white light scattering spectrum obtained from a single nanowire. The scattering spectrum depends on the extinction of the wire, and thus provides information about the frequency dependence of the plasmon resonance. When the plasmon resonance is driven with light polarized along the short axis of the wire a broad scattering spectrum that spans visible and the near infrared is observed.<sup>7</sup> Whenever the system is driven with polarized along the wire's long axis, no clear plasmon absorption is seen. These linear scattering spectra reveal that the plasmon resonance is polarized along the short axis of the wire (transverse surface plasmon), and that its frequency dependence extends over a wide range of the visible/NIR.

Figure 3 depicts the spectral response of the wire when subjected to pump (817 nm) and Stokes (1064 nm) illumination. A broad spectral emission is seen, which is attributed to plasmon enhanced, two-photon excitation of d-band electrons to unoccupied sp states of gold, followed by electron-hole recombination accompanied by photon emission.<sup>8</sup> The two-photon excited luminescence is a characteristic incoherent emission of nano-sized gold. In addition to this incoherent emission, several coherent contributions are observed: second harmonic generation (SHG), sum frequency generation (SFG) and a four wave-mixing signal at the anti-Stokes wavelength. Here, we will be interested in the coherent anti-Stokes signal as a probe for the electronic properties of gold nanowires.

#### 4. COHERENT NONLINEAR OPTICAL PROPERTIES OF GOLD NANOWIRES

Similar to the linear scattering signal, the coherent anti-Stokes (CAS) four wave-mixing signal is dependent on the orientation of the nanowire. In Figure 4 the polarization dependence of the CAS signal is shown. If the polarization is perpendicular with the long axis of the wire ( $\theta = 90^\circ$ ), strong signals are observed. Weaker signals are seen when the angle between the incident beam polarization and the short axis of the wire is changed, with the minimum signal measured at  $\theta = 0^\circ$ . The polarization dependence shows a  $\sin^6 \theta$  dependence. These observations confirm the following: 1) The nonlinear signal is aligned with the orientation of the surface plasmon resonance and 2) the anti-Stokes signal results from a third order interaction with the material. Taken together, these measurements strongly suggest that the detected emission originates from the nonlinear electron motions of the plasmon resonance. In other words, the surface plasmon itself is the primary nonlinear emitter in this experiment, driven directly by the incident radiation that overlaps with the spectrum of the plasmon resonance.

The CAS signal is a measure of the strength of the plasmon resonance. Larger CAS signals are expected for stronger plasmon resonances, which are, in turn, associated with stronger local fields. The CAS signal can thus be compared with the local field enhancement factor to the third order. In Figure 5 such a comparison is made, based on the local field enhancement predicted by the lightning rod model.<sup>8</sup> The graph shows that, for a wire of width 200 nm, the local field is strongly dependent on the height of the wire. Consequently, the changing

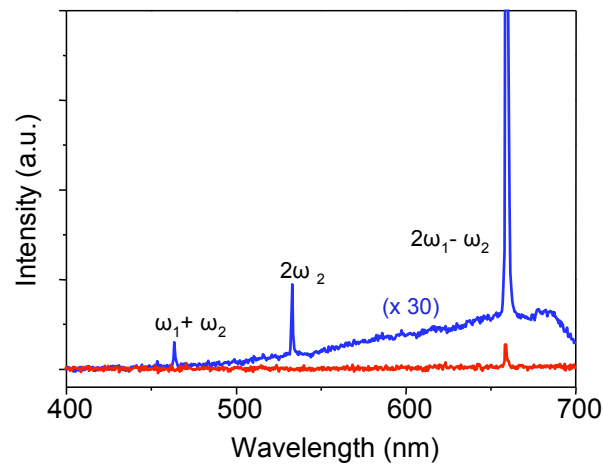


Figure 3. Nanowire emission observed when illuminating the wire with a pump ( $\omega_1$ ) and Stokes ( $\omega_2$ ) beams. Next to a coherent anti-Stokes four-wave-mixing contribution ( $2\omega_1 - \omega_2$ ), a second harmonic generation ( $2\omega_2$ ), a sum frequency generation ( $\omega_1 + \omega_2$ ), and a broad two-photon excited luminescence contribution are observed. Both pump and Stokes beams are  $\sim 10$  ps pulse trains with an average power less than 1 mW.

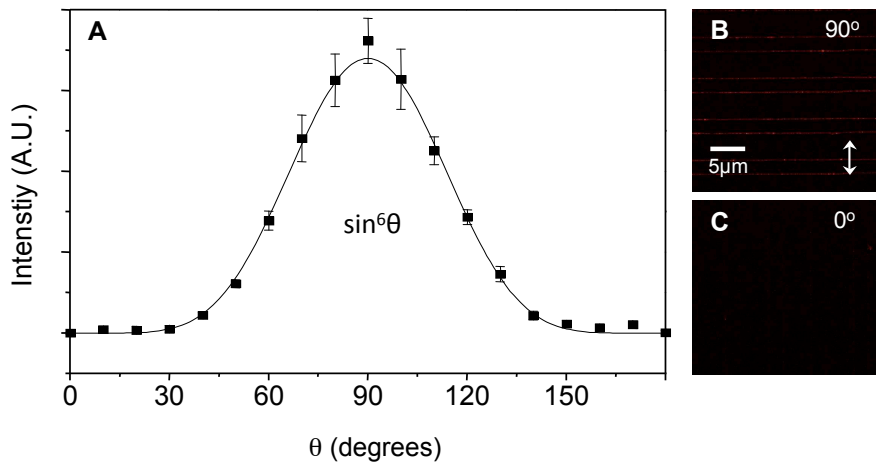


Figure 4. Coherent anti-Stokes four-wave-mixing signal of a gold nanowire ( $w = 188$  nm;  $h = 74$  nm) as a function of orientation relative to the polarization of the pump and Stokes beams.

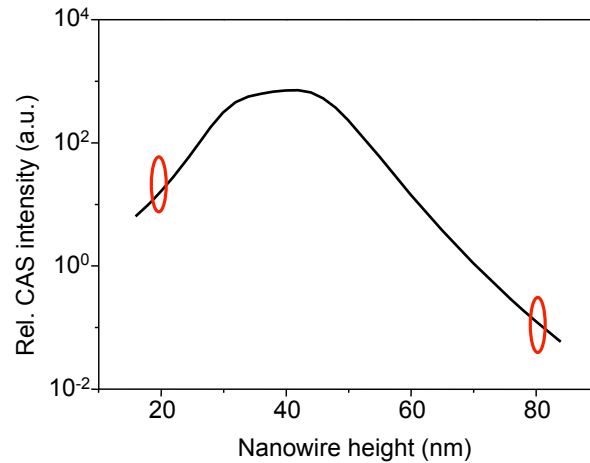


Figure 5. Coherent anti-Stokes four-wave-mixing signal of a gold nanowire ( $w = 188$  nm;  $h = 74$  nm) as a function of orientation relative to the polarization of the pump and Stokes beams.

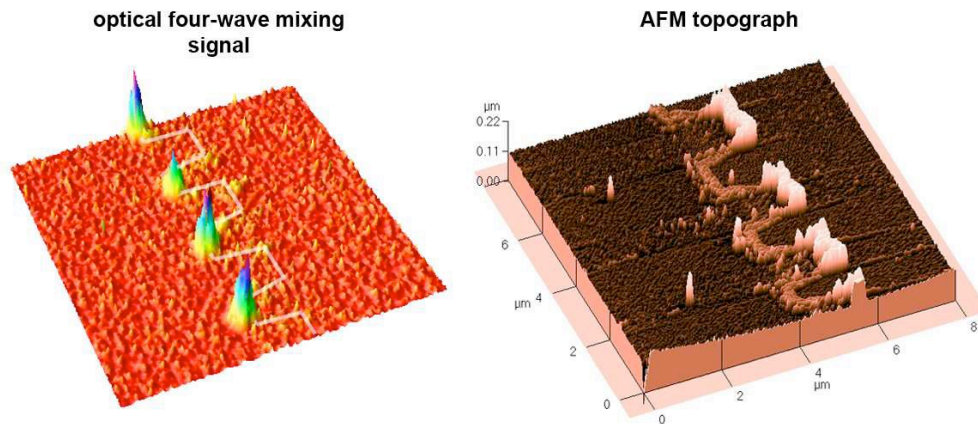


Figure 6. Coherent anti-Stokes image (left) and atomic force microscopy topograph (right) of a gold nanowire sample. This zig-zag nanowire exhibits alternating plateaus with heights of 20 nm and 80 nm, respectively. Note that the higher third order coherent signals from the wire are obtained from the lower plateaus, indicating a stronger electronic plasmon resonance in those regions.

local field enhancement predicts a height-dependence for the CAS signal. The nonlinear coherent response of the plasmon resonance is thus expected to be highly dependent on the dimensions (aspect ratio) of the wire.

This is indeed observed for nanowires of alternating heights. Figure 6 depicts a zig-zag gold nanowire with an average width of 200 nm but with a height that alternates between 20 nm and 80 nm. Based on the local field calculation given in Figure 5, a much stronger signal is predicted for the lower height relative to the high plateaus. The observed CAS four-wave-mixing signal follows the predicted trend. While the height difference between the plateaus only differs by a factor of 4, the CAS signal changes by almost two orders of magnitude. The fact that the highest signals are obtained from the thinner part of the wire confirms that the signal does *not* scale with the amount of material. Rather, the CAS response scales with the strength of the surface plasmon resonance, which is stronger for the lower part of this zig-zag nanowire.

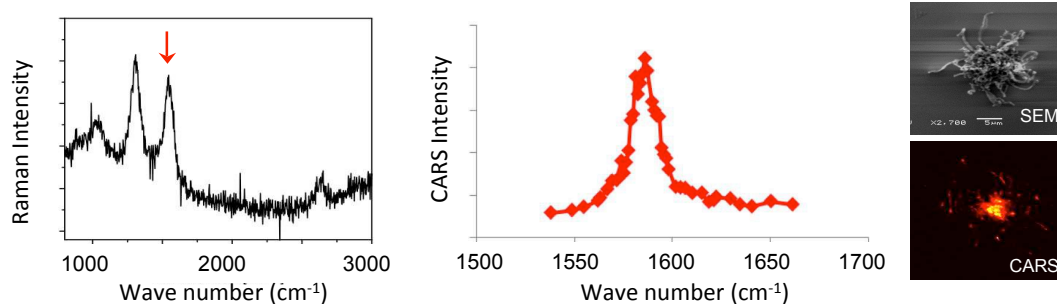


Figure 7. Raman (left) and CARS (right) spectra of carbon nanotubes. The red arrow in the Raman spectrum indicates the location of the G-mode. The CARS spectrum was taken of a nanotube cluster (see insets) near the G-mode ( $1582\text{ cm}^{-1}$ ) of the carbon nanotube.

## 5. COHERENT ANTI-STOKES EMISSION FROM SINGLE CARBON NANOTUBES

Single walled carbon nanotubes are quasi one-dimensional nanoscopic systems composed of a network of  $sp^2$  bonded carbon atoms and with diameters in the 1 nm range.<sup>9</sup> The electronic properties of nanotubes can be either metallic or semiconducting depending on the configuration of the carbon lattice. Electronic transitions induced by visible and near infrared radiation are commonly understood as excitonic.<sup>10</sup> Ensemble absorption experiments have shown that the main optical transitions are oriented along the long axis of the nanotube,<sup>11</sup> a finding confirmed with Rayleigh scattering, fluorescence and resonant Raman experiments in single nanotubes.<sup>12,13</sup> Although nonlinear coherent signals from nanotubes have been observed in ensemble measurements, it is unclear if these systems are conducive of generating detectable nonlinear coherent signals on a single nanotube level.

The ability to detect nonlinear coherent signals from single nanotubes would not only reveal information on the orientation and the heterogeneity of the optical nonlinearity, it would also provide a potential model system for studying the fundamentals of the nonlinearity of single transitions.<sup>14</sup> Carrying out four-wave-mixing experiments by detecting the coherent anti-Stokes signatures of the electronic transitions is a sensitive approach to achieve single nanotube nonlinear spectroscopy.

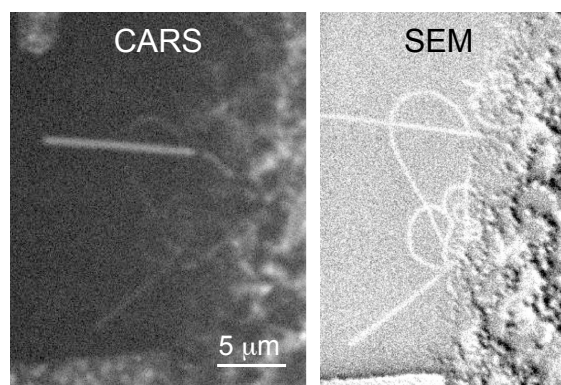


Figure 8. Coherent anti-Stokes imaging of a single carbon nanotube at  $1582\text{ cm}^{-1}$ . Several tubes can be discerned, along with the nanoparticle catalysts from which the nanotubes grow (right side of image). A corresponding scanning electron micrograph is provided for comparison.

Here we investigate the coherent anti-Stokes response from single nanotubes. We have fabricated single wall carbon nanotubes (SWNT) through catalyst controlled chemical vapor deposition on quartz substrates.<sup>15</sup> In Figure 7 the spectral dependence of anti-Stokes signal is shown for a microscopic cluster of nanotubes. Such clusters are composed of both metallic and semiconducting nanotubes, in addition to remnant amorphous carbon. The anti-Stokes signal shows a clear dependence on graphite mode at  $1582\text{ cm}^{-1}$  (G-band), which is also confirmed

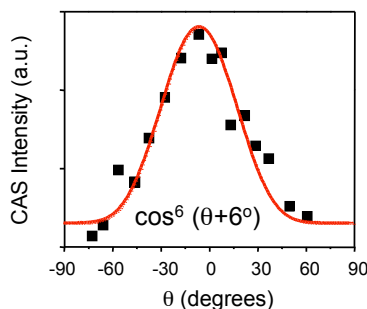


Figure 9. The polarization dependence of the CAS signal obtained from a single nanotube.

by the Raman spectrum. In addition to the vibrational resonant signal, the purely electronic contribution can be seen.

The brightness of the nanotubes on a single molecule level depends on the electronic properties of the nanotube. In Figure 8 the coherent anti-Stokes signal of several nanotubes is resolved. The location of the nanotubes is confirmed by the scanning electron micrograph. The signal from the bright nanotube depends on the presence of both the pump (911 nm) and Stokes (1064 nm). Tuning the pump beam yields only a minimal change of the anti-Stokes signal, indicating that the response originates predominantly from the electronic contribution of the tube. No multi-photon excited luminescence contributions were detected at this setting of the incident beams. Whereas the signal from one nanotube is bright, the response from other tubes is significantly less strong, which is a direct reflection of the heterogeneity of the electronic properties of the nanotubes in the ensemble.

In Figure 9 we investigate the nature of the electronic resonance. By rotating the nanotube, a  $\cos^6\theta$  dependence is observed. The brightest signals are observed when the polarization of the pump and Stokes beams are along the long axis of the nanotube. Similar observations have been made for fluorescence excitation and Rayleigh scattering, suggesting that the excitonic resonance polarized along the long axis is also responsible for the observed coherent nonlinear signal.

## 6. CONCLUSION

In this work, we have used the electronic response associated with a coherent anti-Stokes measurement to study the nonlinear optical properties of electronic resonances in nanoscopic systems. The coherent anti-Stokes signal is an excellent probe for the nonlinearity of the plasmon resonances in metallic nanostructures, among which nanowires. In addition, the coherent anti-Stokes signal proved successful in resolving single carbon nanotubes. This probe was used to determine the orientation of the electronic transitions that are on resonance with the excitation beams. The observation of nonlinear coherent signals from single molecular systems is encouraging, as it sets the stage for more fundamental investigations of nonlinear optics in the single molecule limit.

## REFERENCES

- [1] Evans, C. L. and Xie, X. S., “Coherent anti-stokes raman scattering microscopy: chemical imaging for biology and medicine,” *Annu. Rev. Anal. Chem.* **1**, 883–909 (2008).
- [2] Chen, C. K., de Castro, A. R. B., and Shen, Y. R., “Surface coherent anti-stokes raman scattering spectroscopy,” *Phys. Rev. Lett* **43**, 946–949 (1979).
- [3] Chemla, D. S., Heritage, J. P., Liao, P. F., and Isaacs, E. D., “Enhanced four-wave mixing from silver particles,” *Phys. Rev. B* **27**, 4553–4558 (1983).
- [4] Danckwerts, M. and Novotny, L., “Optical frequency mixing at coupled gold nanoparticles,” *Phys. Rev. Lett.* **98**, 026101–026104 (2007).
- [5] Kim, H., Taggart, D. K., Xiang, C., Penner, R. M., and Potma, E. O., “Spatial control of coherent anti-stokes emission with height-modulated gold zig-zag nanowires,” *Nano Lett.* **8**, 2373–2377 (2008).
- [6] Menke, E. J., Thompson, M. A., Xiang, C., Yang, L. C., and Penner, R. M., “Lithographically patterned nanowire electrodeposition,” *Nature Mat.* **5**, 914–919 (2006).

- [7] Kim, H., Xiang, C., Guell, A. G., Penner, R. M., and Potma, E. O., “Tunable two-photon excited luminescence in single gold nanowires fabricated by lithographically patterned nanowire electrodeposition,” *J. Phys. Chem. C* **112**, 12721–12727 (2008).
- [8] Boyd, G. T., Yu, Z. H., and Shen, Y. R., “Photoinduced luminescence from noble metals and its enhancement on roughened surfaces,” *Phys. Rev. B* **33**, 7923–7936 (1986).
- [9] Saito, R., Dresselhaus, G., and Dresselhaus, M. S., [*Physical Properties of Carbon Nanotubes*], Imperial College Press, London (1998).
- [10] Wang, F., Dukovic, G., Brus, L. E., and Heinz, T. F., “The optical resonances in carbon nanotubes arise from excitons,” *Science* **308**, 838–841 (2004).
- [11] Jiang, K., Li, Q., and Fan, S., “Nanotechnology: spinning continuous carbon nanotube yarn,” *Nature* **419**, 801 (2002).
- [12] Sfeir, M. Y., Wang, F., Huang, L., Chuang, C. C., Hone, J., O’Brien, S. P., Heinz, T. F., and Brus, L. E., “Simultaneous fluorescence and raman scattering from single carbon nanotubes,” *Science* **301**, 1354–1356 (2003).
- [13] Hartschuh, A., Pedrosa, H. N., Novotny, L., and Kraus, T. D., “Simultaneous fluorescence and raman scattering from single carbon nanotubes,” *Science* **301**, 1354–1356 (2003).
- [14] Marx, C. A., Harbola, U., and Mukamel, S., “Nonlinear optical spectroscopy of single, few, and many molecules: nonequilibrium green’s function qed approach,” *Phys. Rev. A* **77**, 022110 (1–14) (2008).
- [15] Goldsmith, B., Coroneus, J. G., Khalap, V. R., Kane, A. A., Weiss, G. A., and Collins, P. G., “Conductance-controlled point functionalization of single-walled carbon nanotubes,” *Science* **315**, 77–81 (2007).